Efferent axonal projections of the habenular complex in the fire-bellied toad *Bombina orientalis*

Frédéric Laberge* and Allison Smith

Department of Integrative Biology, University of Guelph

*Correspondence to: F. Laberge, Department of Integrative Biology, University of Guelph, 50 Stone Road East, Guelph, ON, Canada N1G 2W1. Tel.: 1-519-824-4120 ext. 56238, Fax: 1-519-767-1656, e-mail: flaberge@uoguelph.ca

Running head: Habenular projections in the fire-bellied toad

With 5 figures and 3 tables

Keywords: amphibians, habenula, asymmetry, axons, biocytin, anterograde tracing, retrograde tracing

Abstract

The habenular complex and its associated axonal pathways are often thought of as phylogenetically conserved features of the brain among vertebrates despite the fact that detailed studies of this brain region are limited to a few species. Here, the gross morphology and axonal projection pattern of the habenular complex of an anuran amphibian, the fire-bellied toad *Bombina orientalis*, was studied to allow comparison with the situation in other vertebrates. Axonal pathways were traced using biocytin applications in dissected brain preparations. The results show that the rostral part of the left dorsal nucleus is enlarged in this species, while the rostral ventral nucleus and caudal parts do not show left-right size differences. Biocytin applications revealed widespread axonal projections of the habenular complex to the posterior tuberculum/dorsal hypothalamic region, ventral tegmentum, interpeduncular nucleus (IPN), and raphe median. Additionally, axons targeting the lateral hypothalamus originated from the ventral habenular nuclei. The results also suggest an asymmetrical pattern of projection to the IPN in the rostral part of the habenular complex, where the left habenula targeted preferentially the dorsal IPN while the right habenula targeted preferentially the ventral IPN. The caudal habenular nuclei showed no asymmetry of projections as both sides targeted the ventral IPN. Comparison of the habenular complex axonal connectivity across vertebrates argues against strong phylogenetic conservation of the axonal projection patterns of different habenular nuclei.

1. Introduction

The habenula is a brain structure found in the dorsal diencephalon, or roof part of prosomere 2 according to the prosomeric model of brain development (Puelles and Rubenstein 2003). This brain region has recently been implicated in the processing of information related to aversive events (Matsumoto and Hikosaka 2009; Stamatakis and Stuber 2012; Amo et al. 2014; Lawson et al. 2014; Hennigan et al. 2015). The habenula often displays left-right asymmetry in size, neurochemistry and/or connectivity (Concha and Wilson 2001; Villalón et al. 2012). Medial and lateral nuclei have been recognized in the habenular complex of mammals, and these nuclei can be further subdivided into subnuclei based on connectivity or neurochemistry (Herkenham and Nauta 1977; 1979; Andres et al. 1999; Geisler et al. 2003; Aizawa et al. 2011; Wagner et al. 2014). Nuclei homologous to the mammalian medial and lateral nuclei have been proposed in the habenular complex of other vertebrate groups (Kemali and Làzàr 1985; Amo et al 2010; Aizawa et al 2011; Stephenson-Jones et al 2012).

Across vertebrates, the habenular complex and its projections are thought to be very conservative features of the brain (Butler and Hodos 1996). However, this claim is based on few examples of detailed studies of habenular complex anatomy in different vertebrates. For example, studies providing an account of the axonal projections of the different habenular nuclei are limited to laboratory rodents (Herkenham and Nauta 1979; Kim 2009; Quina et al. 2015), one species of lizard (Distel and Ebbesson 1981), the zebrafish (Aizawa et al. 2005; Amo et al. 2010), and one species of lamprey (Stephenson-Jones et al. 2012). Efferent projections of the avian habenular complex have not been studied and studies in amphibians are incomplete (see below). Despite this paucity of studies, differences in habenular complex axonal projection patterns have already been noted across vertebrates. First, Bianco and Wilson (2009) observed

62 that the lateral habenular nuclei appear to show a less evolutionarily conserved pattern of axonal
63 projections compared to the medial habenular nuclei. Second, Kuan et al. (2007) proposed that
64 the dorsoventral asymmetry of the habenula to midbrain projection is a unique feature of teleost
65 fishes. Thus, evolutionary changes in the habenular complex could have been underestimated
66 and studies of representative species within understudied groups of vertebrates could prove
67 helpful in understanding the evolution of habenular complex connectivity.
68 The present study aimed to characterize in detail the axonal projections of the habenular
69 complex in an amphibian, the anuran *Bombina orientalis*, in order to compare with other
70 vertebrate groups. *B. orientalis* is particularly interesting for this purpose because it belongs to a
71 basal group in anuran phylogeny (Pyron and Wiens 2011) and could provide useful information
72 to elucidate the tetrapod brain morphotype (e.g. Northcutt 1995) when considering that the more
73 basal caecilians and urodeles underwent substantial secondary brain simplification during their
74 evolutionary history (Roth et al. 1997; Schmidt and Wake 1997). Experimental studies of
75 habenular complex connections have previously been conducted in the frog *Rana esculenta*
76 (Kemali et al. 1980; Kemali and Guglielmotti 1982; Kemali and Làzàr 1985; Guglielmotti and
77 Fiorino 1998), but a precise picture of the projection patterns of different nuclei has yet to be
78 achieved in any amphibian species. In frogs, the habenular complex displays dorsal and ventral
79 nuclei on each side of the brain and the left dorsal nucleus shows conspicuous lateral and medial
80 divisions. The studies of *R. esculenta* concluded that both dorsal and ventral nuclei send axonal
81 projections to the interpeduncular nucleus (IPN) and some axons continue their course caudally
82 beyond this brain region. However, the region of termination of these axons has not been
83 identified. Kuan et al. (2007) also showed that the dorsal habenula of larval amphibians (anuran
84 *Rana clamitans* and urodele *Ambystoma maculatum*) send axons to the IPN. There remains a

need to ascertain the targets of axons projecting beyond the IPN in amphibians and to verify the presence or absence of projections to the hypothalamus and rostral ventral midbrain present in other vertebrates (e.g. rat: Herkenham and Nauta 1979; lizard: Distel and Ebbesson 1981; lamprey: Stephenson-Jones et al. 2012). This was attempted by using tract tracing of habenular pathways with biocytin; a sensitive tracer substance that can be used for precise applications in *in vitro* brain preparations of amphibians.

2. Materials and methods

Animals

Forty-six adult fire-bellied toads of mixed sexes were used in the present study. The animals were bought from a local supplier (National Reptile Supply, Mississauga, ON) and held at a temperature of 21°C under a photoperiod of 12:12-h light:dark (lights on at 7:00h). The toads were housed in groups in glass tanks (37 × 22 × 25 cm) with gravel substrate, broken clay pots, and flat stones for cover. They had continuous access to water and were fed crickets (*Acheta domesticus*) lightly dusted with calcium and vitamin powder *ad libitum* once weekly. The experimental procedures were approved by the University of Guelph animal care committee under the guidelines of the Canadian Council on Animal Care.

Procedures

All experiments were carried out *in vitro* in isolated brain preparations. After deep anaesthesia by immersion in a solution of 0.1% tricaine methanesulfonate (Argent Chemical Laboratories, Redmond, WA), the animals were quickly decapitated, the lower jaw was removed, and the skull was opened from the roof of the mouth to enable brain dissection. The dissection was performed

in Ringer's solution consisting of Na^{+} 129 mM, K^{+} 4 mM, $Ca2^{+}$ 2.4 mM, $Mg2^{+}$ 1.4 mM, Cl^{-} 115 mM, $HCO3^{-}$ 25 mM, glucose 10 mM, bubbled with 95% O^{2}/5% CO^{2} until a pH of 7.3 was achieved. Tract tracing of neural pathways was achieved in two ways: 1) by manual application of biocytin crystals (Sigma-Aldrich B4261, St. Louis, MO) directly to the lightly lesioned surface of the brain outside of the Ringer's bath, and 2) by iontophoretic injection of a 2% solution of biocytin dissolved in 0.3M KCl. Lesioning of the brain surface was achieved using a pulled glass pipette with a broken tip. Iontophoresis was achieved by loading a pulled glass pipette (tip broken at 10-15 µm) with the solution and passing a pulsed current of 4 µA (on/off every 5s) for 10-20 min. Additionally, labeling of single neurons by intracellular injections of the 2% biocytin solution was conducted in an attempt to clarify some axonal projection patterns. For the latter, brains were pinned down in a chamber perfused with oxygenated Ringer's solution (6 ml/min) and pulled micropipettes with sharp tips were advanced in brain tissue while a 200 msec hyperpolarizing current of 0.2 nA was applied every second. Current was injected and potential was monitored using an electrometer (Duo 773, World Precision Instruments, Sarasota, FL,USA). Electrode impedance ranged between 80-120 MΩ. Penetration of neurons was identified by rebound action potential activity and followed by injection of biocytin by passing a pulsed current of 1 nA for 4 min.

After biocytin applications, the brains were stored in oxygenated Ringer's solution for 5-6 hours at room temperature and then at 4°C overnight. On the next day, the brains were fixed in 2% paraformaldehyde and 2% glutaraldehyde, and then 50-µm-thick transverse sections were cut on a VT1200 vibrating microtome (Leica Biosystems, Wetzlar, Germany). Biocytin was visualized by means of an avidin-biotin horseradish peroxidase complex (Vector Laboratories, Burlingame, CA) by using diaminobenzidine (Sigma) as chromogen with heavy metal

intensification achieved by adding 0.03% nickel sulphate and cobalt chloride to the solution (Adams, 1981). Sections were lightly counterstained with cresyl violet, dehydrated in ethanol, cleared in xylene, and coverslipped before examination under the microscope.

Analysis

The assessment of biocytin application sites and charting of retrograde labeling and axonal projections was done using a DM1000 light microscope equipped with a drawing tube (Leica). The intensity of axonal projections and retrograde labeling was assessed qualitatively by a single observer (FL). Axonal projections were described as notable or weak, with weak labeling corresponding to the presence of only one or two axons with limited varicosities in a given brain region and notable labeling corresponding to the presence of multiple axons with abundant varicosities along their length in a brain region. Retrograde labeling was described as strong, moderate or weak depending on the number of cell bodies labeled in a given brain region, as exemplified in Figure S1. Photomicrographs were scanned using an Eclipse 90i upright microscope (Nikon, Tokyo, Japan) equipped with a Retiga 2000R digital camera (QImaging, Surrey, BC), modified (sized and cropped) and optimized for presentation (brightness and contrast) using Adobe Photoshop CS3 (Adobe Systems, San Jose, CA). Analysis of potential asymmetry of the habenular complex was done by measuring the surface area of habenular divisions on serial sections using the contour drawing function in Neurolucida version 11.02.1 (MBF Bioscience, Williston, VT, USA) on the Eclipse 90i microscope. Surface areas were converted to volumes by multiplying values by section thickness. Comparison of the left and right habenular volumes involved all sections comprising the habenular complex. Such comparison of the rostral habenula involved the 4 most rostral sections, while the caudal

habenula involved the 3 most caudal sections. Statistical analyses were done in Prism version 5.04 (GraphPad Software Inc., San Diego, CA). The neuroanatomical framework used for presentation of the data is based on published accounts in *Rana perezi* (Puelles et al. 1996), *Rana catesbeiana* (Neary and Northcutt 1983), and the fire-bellied toad (Laberge and Roth 2007; Laberge et al. 2008).

3. Results

Asymmetry of habenular complex

Figure 1 illustrates the extent of the habenular complex in the fire-bellied toad brain. The specimen chosen for this purpose received a large application of biocytin that covered part of the ventral tegmentum (vTEG) and the dorsoventral extent of IPN and rostral raphe median (mRaphe). The abundant retrograde labeling that resulted from this tracer application allowed a clear outline of the extent of the habenular complex. The labeling shows equivalent staining in the left and right caudal habenula, but more prominent staining in the left rostral habenula. The higher magnification inset included in Figure 1F shows details of the dorsal and ventral nuclei on each side of the brain as well as the lateral and medial divisions visible in the middle left dorsal habenula nucleus. Such divisions in the left dorsal habenula nucleus were also noted in the frog *Rana esculenta* (Kemali and Làzàr 1985; Guglielmotti and Fiorino 1998). The dorsal nuclei (especially in their middle part) are structured as cellular rims surrounding central neuropils, while ventral nuclei are made of homogeneously distributed cell bodies. Note that there is high inter-individual variability in the divisions of the dorsal habenular nuclei in their middle part.

Five specimens displaying abundant retrograde labeling in the habenular complex were chosen for morphometric analysis of the habenular nuclei on each side of the brain. Note that the

volumes of the lateral and medial divisions in the middle left dorsal habenula nucleus were not calculated because their boundaries were difficult to estimate. A two-tailed paired t-test showed that the volume of the left habenula (0.017 ± 0.0009 mm^3; mean ± standard deviation) is larger than the right habenula (0.013 ± 0.0008 mm^3; $t_4 = 15.8$, $P < 0.0001$). Further analysis showed no difference between volumes of the left and right caudal habenula (left caudal: 0.0032 ± 0.0005 mm^3, right caudal: 0.0027 ± 0.0006 mm^3; $t_4 = 1.7$, $P = 0.18$) or rostral ventral habenula (left rostral ventral: 0.0042 ± 0.0003 mm^3, right rostral ventral: 0.0044 ± 0.0003 mm^3; $t_4 = 1.2$, $P = 0.30$). However, volume of the left rostral dorsal habenula (0.005 ± 0.0005 mm^3) was larger than the right rostral dorsal habenula (0.002 ± 0.0004 mm^3; $t_4 = 13.9$, $P = 0.0002$). Therefore, left-right asymmetry of the habenular complex in the fire-bellied toad is the result of an enlarged rostral part of the dorsal nucleus on the left side.

Efferent axonal projections of the habenular complex

Figure 2 shows a typical example of the axonal projections revealed by biocytin applications directly to the habenular nuclei. In this case, the tracer application involved both dorsal and ventral nuclei along most of the rostrocaudal extent of the habenula on the left side of the brain (Figure 2 A-B, B'). Output axons of the habenular nuclei form the fasciculus retroflexus, which runs from the dorsal diencephalon to the posterior tuberculum and dorsal hypothalamus region on the side ipsilateral to the application site (Figure 2C). Some axonal varicosities are observed near the rostral vTEG and caudal dorsal hypothalamus, but no clear axon branches are seen there (Figure 2D). Abundant varicose axons were seen in the ventral IPN at a more rostral level (Figure 2E) and both ventral and dorsal IPN more caudally in this case (Figure 2F). Finally, varicose axons extended caudally into the ventral part of mRaphe of the medulla oblongata

(Figure 2G). Axons cross over the brain midline multiple times to invade both sides of IPN and they maintain this central, bilateral location in mRaphe.

Table 1 summarizes the results of sixteen anterograde labeling experiments. The extent of these biocytin applications sites is detailed in Figure S2. The majority of biocytin applications to the habenular complex revealed consistent axonal projections to the posterior tuberculum/dorsal hypothalamus region (Figure 3B), rostral vTEG (Figure 3C), IPN (Figure 3D-E) and mRaphe (Figure 3F). Projections to mRaphe were limited to the anterior part of this region. Axonal projections to the contralateral habenula neuropil were often seen, but no obvious pattern suggesting a topographic organization emerged when comparing different applications. Projections to the lateral hypothalamus (lHYP; Figure 3A), and possibly the preoptic area (POA), appear to originate from the ventral habenular nuclei, when taking into account the potential projections due to inclusion in some application sites of parts of the dorsal thalamus which are known to send axons to lHYP/POA (Laberge et al. 2008). Axons found in the commissural pretectum and the median thalamic neuropil may also be due to inclusion of parts of the thalamus in some application sites, but this problem would require further investigation due to a limited sample size of applications displaying such connections.

An asymmetric pattern of axonal projections to the IPN was noticed: while applications to the caudal habenula targeted the ventral part of IPN, applications to the rostral part of the habenula showed a left-right side difference. The rostral habenula on the left side targeted preferentially the dorsal IPN (Figure 3D), while the rostral habenula on the right side targeted preferentially the ventral IPN (Figure 3E). This pattern is reminiscent of the dorsoventral asymmetry of projections of left and right dorsal habenulae in zebrafish (Aizawa et al. 2005; Amo et al. 2010) and contrasts with the symmetrical habenular projections to IPN seen in larval

amphibians (Kuan et al. 2007). This dorsoventral asymmetry of projections to IPN in the fire-bellied toad was confirmed by intracellular labeling of neurons. In one case, one neuron with its cell body in the rostral part of the left dorsal habenula sent two axons (or axon collaterals) into the ipsilateral fasciculus retroflexus and targeted the whole rostrocaudal extent of IPN in its dorsal part (Figure 4A). In another case, two neurons labeled by the same intracellular injection had their cell bodies in the rostral part of the right dorsal habenula and sent axons that ended in the ventral part of IPN (Figure 4B). Few successful intracellular injections of habenular complex neurons were obtained due to difficulties with intracellular recording in this brain region using a dorsal approach in intact brain preparations.

Biocytin is also taken up at synaptic sites and moved back toward the cell body to produce retrograde labeling of neurons. Retrograde labeling resulting from applications of biocytin to the habenular complex is summarized in Table S1. This analysis showed that the main afferent brain region to the habenular complex in the fire-bellied toad is the bed nucleus of the pallial commissure/thalamic eminence continuum (12 out of 16 applications); a projection that was previously described in Laberge and Roth (2007). In this previous work, a ventrolateral thalamic cell group was additionally retrogradely labeled following large tracer applications to the habenular complex. However, retrograde labeling in the ventrolateral thalamus was only seen in 4 large tracer applications out of 16 in the present study, suggesting that afferents from the ventrolateral thalamic cell group might be circumscribed to a small portion of the habenular complex or that they terminate or travel nearby the habenula without entering it.

Table 2 shows retrograde labeling of neurons in the habenular complex following biocytin applications to other brain regions (n = 21 experiments). The extent of these biocytin applications sites is detailed in Figure S3 and the qualitative scale of retrograde labeling intensity

is illustrated by an example in Figure S1. These results confirm the strong connection between the caudal habenula and the IPN/mRaphe. In accordance with the projection pattern described above, applications lateral to the IPN or in the caudal part of mRaphe did not label any neurons in the habenular complex. The results also confirm a moderate projection of the ventral nuclei to lHYP. Applications restricted to the preoptic area and suprachiasmatic hypothalamic nucleus – just rostral of lHYP – or the ventral thalamus – just dorsal of lHYP – did not produce any retrograde labeling in the habenular complex. Additionally, retrograde labeling experiments suggest a strong projection of the rostral ventral habenular nuclei to mRaphe. Finally, it should be noted that retrograde labeling in the rostral dorsal habenula was strongest in the tracer application that involved the dorsal IPN, which is hard to reach when applying crystalline biocytin on the surface of the brain.

4. Discussion

Figure 5 summarizes the axonal projections of the habenular complex in the adult fire-bellied toad. The variation in axonal projections between habenular nuclei involves both left-right differences in innervation of the IPN and differences between the dorsal and ventral nuclei in innervation of lHYP. The results also suggest extensive overlap of axonal projections between nuclei. The morphological asymmetry of the anuran habenular complex detected previously (Kemali and Làzàr 1985; Guglielmotti and Fiorino 1998) and in our analysis is restricted to the rostral part of the dorsal nucleus.

Methodological considerations

The amount of retrograde labeling following biocytin applications depended on the depth of lesions made to the brain surface in the case of crystalline applications, and whether more than one region was included in the application site in all cases. Conclusions reached here were inferred from consistent patterns between different applications and the use of both anterograde and retrograde tracing for confirmation of connections between brain regions.

One projection site from the habenular complex that proved difficult to confirm in the fire-bellied toad is lHYP. All anterograde tracing experiments where varicose axons were seen in lHYP or POA, except one, involved retrograde labeling of neurons located in the ventral thalamus. It is possible that retrogradely labeled neurons in the ventral thalamus could send axons to lHYP, rather than neurons of the habenular complex. However, we reject this possibility because tracer injections in the ventral thalamus itself, in its medial or lateral parts, did not result in retrograde labeling in the habenular complex. Overall, evidence from biocytin applications involving the preoptic area, suprachiasmatic nucleus, and lHYP suggest that only the caudal parts of lHYP receive axonal input from the habenular complex, and that this input is limited to the ipsilateral ventral nuclei.

Comparison of habenular complex efferents across vertebrates

The present study clarified and expanded the known habenular complex axonal projection sites in anuran amphibians. If the results in the fire-bellied toad are broadly applicable to the situation in other anurans, then in addition to the IPN (Kemali and Làzàr 1985; Kuan et al. 2007), the anuran habenular complex also targets lHYP, the posterior tuberculum/dorsal hypothalamus region, rostral vTEG, and rostral mRaphe. The projection to mRaphe was anticipated from the finding of habenula axons projecting beyond the IPN in *Rana esculenta* by Kemali and Làzàr

(1985). The results in fire-belied toad also suggest that the topography of habenular complex axonal projections to IPN is variable within amphibians. The symmetric IPN innervation by right and left dorsal habenulae shown by Kuan et al. (2007) differs from the IPN dorsoventral innervation topography of the rostral habenular nuclei seen here. Since Kuan et al. (2007) studied larval amphibians and newborn mice, it is unclear if this difference is due to ontogenetic difference in IPN innervation patterns or species differences. Nevertheless, this finding suggests that a distinct dorsoventral patterning of left and right habenular projections to IPN is not unique to teleosts. However, our confirmation of distinct rostral habenular projections to the ventral and dorsal IPN obtained by anterograde labeling in the fire-bellied toad is limited to retrograde labeling from a single application to the deep IPN and two intracellular injections. Further experiments such as tracer applications restricted to the dorsal and ventral IPN would be needed for convincing confirmation of the dorsoventral asymmetry of this projection in adult amphibians.

Considering that the habenular complex and its projections are thought of as conservative features of the brain across vertebrates, the plesiomorphic (or basal) state of habenular projection patterns should be easy to determine. However, when comparing known axonal targets of the habenular complex across vertebrates in a phylogenetic context (Table 3), some difficulties arise. Namely, there are fewer targets, and distinct targets between habenular nuclei, in lampreys and teleosts compared to amphibians (see Table 3 for references). Additionally, both habenular nuclei show differences in axonal targets across groups, arguing against the proposal of Bianco and Wilson (2009) suggesting that medial habenular nuclei show a more conservative evolutionary pattern in vertebrates. A reconsideration of the habenular complex as a vertebrate brain region with more labile axonal connections invites different evolutionary scenarios. In one

scenario, the patterns of habenular complex efferents in fish could be derived features evolved from more widespread ancestral habenular projections, the latter of which would have been kept in amphibians. Habenular complex projections are especially simpler in teleosts, where they are limited to a single brain region for each habenula nucleus (Amo et al. 2010). The divergent topography of habenular projections to IPN between lampreys (rostrocaudal topography) and teleosts (dorsoventral topography) also suggests that habenular projection patterns in fish saw some evolutionary changes. In an alternative scenario, ancestral amphibians would have gained many habenula axonal targets compared to the simpler situation in fish, and from there evolution would have again refined the projections of the medial and lateral habenular nuclei to a set of specific brain regions in amniotes (here, lizards and rodents for which we have data). A final evolutionary scenario posits that the lineage leading to modern amphibians, not the common ancestor of tetrapods, would have gained many habenula axonal targets. In this regard, it is interesting to note the similarities of habenular complex projections between lampreys and amniotes. Stephenson-Jones et al. (2012) showed that the habenular nuclei in the river lamprey (*Lampetra fluviatilis*) have similarly broad brain targets as in amniotes, with the exception of projections to the raphe, which are absent. In this final scenario, the habenular complex in basal vertebrates would have targeted many brain regions with a distinct pattern between nuclei somewhat similar to the situation in lampreys and amniotes, and from there teleosts saw a reduction in habenula targets, while modern amphibians saw an increase in habenula targets for both the dorsal and ventral nuclei.

Conclusion

The present study expanded the known habenular projection targets in anuran amphibians to include the hypothalamus, tegmentum and median raphe. The breadth of axonal targets shown for both habenular nuclei in the fire-bellied toad is unique among vertebrates that have been studied so far and presents a problem for establishing a plausible scenario for the evolution of habenular complex efferents. The finding suggests that conservation of habenular complex connectivity among vertebrates could have been overestimated, and opens questions about the evolution of this brain structure. More research on the connectivity and neurochemistry of habenular nuclei in animals strategically placed in vertebrate phylogeny will be needed to elucidate this problem. In the meantime, the use of caution is suggested when proposing homologies between brain nuclei in different groups even when dealing with a seemingly conserved structure such as the habenular complex.

Acknowledgments

This research was supported by a NSERC Discovery grant to F. Laberge. The authors thank Irene Yin-Liao for conducting the regional volume measurements used in the analysis of habenula asymmetry. The authors declare no conflict of interest.

References

Adams JC (1981): Heavy metal intensification of DAB-based HRP reaction product. J Histochem Cytochem 29:775.

Aizawa H, Bianco IH, Hamaoka T, Miyashita T, Uemura O, Concha ML, Russell C, Wilson SW, Okamoto H (2005): Laterotopic representation of left-right information onto the dorso-ventral axis of a zebrafish midbrain target nucleus. Curr Biol 15:238-243.

Aizawa H, Amo R, Okamoto H (2011): Phylogeny and ontogeny of the habenular structure. Front Neurosci 5:138.

Amo R, Aizawa H, Takahoko M, Kobayashi M, Takahashi R, Aoki T, Okamoto H (2010): Identification of the zebrafish ventral habenula as a homolog of the mammalian lateral habenula. J Neurosci 30:1566-1574.

Amo R, Fredes F, Kinoshita M, Aoki R, Aizawa H, Agetsuma M, Aoki T, Shiraki T, Kakinuma H, Matsuda M, Yamazaki M, Takahoko M, Tsuboi T, Higashijima S, Miyasaka N, Koide T, Yabuki Y, Yoshihara Y, Fukai T, Okamoto H (2014): The habenulo-raphe serotonergic circuit encodes an aversive expectation value essential for adaptive active avoidance of danger. Neuron 84:1034-1048.

Andres KH, von Düring M, Veh RW (1999): Subnuclear organization of the rat habenular complexes. J Comp Neurol 407:130-150.

Bianco IH, Wilson SW (2009): The habenular nuclei: a conserved asymmetric relay station in the vertebrate brain. Phil Trans R Soc B 364:1005-1020.

Butler AB, Hodos W (1996): Comparative Vertebrate Neuroanatomy: Evolution and Adaptation. New York, Wiley-Liss.

Concha ML, Wilson SW (2001): Asymmetry of the epithalamus of vertebrates. J Anat 199:63-84.

Díaz C, Puelles L (1992): In vitro HRP-labeling of the fasciculus retroflexus in the lizard *Gallotia galloti*. Brain Behav Evol 39:305-311.

Distel H, Ebbesson SOE (1981): Habenular projections in the monitor lizard (*Varanus benegalensis*). Exp Brain Res 43:324-329.

Geisler S, Andres KH, Veh RW (2003): Morphologic and cytochemical criteria for the identification and delineation of individual subnuclei within the lateral habenular complex of the rat. J Comp Neurol 458:78-97.

Guglielmotti V, Fiorino L (1998): Asymmetry in the left and right habenulo-interpeduncular tracts in the frog. Brain Res Bull 45:105-110.

Hennigan K, D'Ardenne K, McClure SM (2015): Distinct midbrain and habenula pathways are involved in processing aversive events in humans. J Neurosci 35:198-208.

Herkenham M, Nauta WJH (1977): Afferent connections of the habenula nuclei in the rat. A horseradish peroxidase study, with a note on the fiber-of-passage problem. J Comp Neurol 173:123-146.

Herkenham M, Nauta WJH (1979): Efferent connections of the habenular nuclei in the rat. J Comp Neurol 187:19-48.

Kemali M, Guglielmotti V (1982): The connections of the frog interpeduncular nucleus (ITP) demonstrated by horseradish peroxidase (HRP). Exp Brain Res 45:349-356.

Kemali M, Làzàr G (1985): Cobalt injected into the right and left fasciculi retroflexes clarifies the organization of this pathway. J Comp Neurol 233:1-11.

Kemali M, Guglielmotti V, Gioffré D (1980): Neuroanatomical identification of the frog habenular connections using peroxidase (HRP). Exp Brain Res 38:341-347.

Kim U (2009): Topographic commissural and descending projections of the habenula in the rat. J Comp Neurol 513:173-187.

Kuan Y-S, Gamse JT, Schreiber AM, Halpern ME (2007): Selective asymmetry in a conserved forebrain to midbrain projection. J Exp Zool 308B:669-678.

Laberge F, Roth G (2007): Organization of the sensory input to the telencephalon in the fire-bellied toad, *Bombina orientalis*. J Comp Neurol 502:55-74.

Laberge F, Mühlenbrock-Lenter S, Dicke U, Roth G (2008): Thalamo-telencephalic pathways in the fire-bellied toad *Bombina orientalis*. J Comp Neurol 508:806-823

Lawson RP, Seymour B, Loh E, Lutti A, Dolan RJ, Dayan P, Weiskopf N, Roiser JP (2014): The habenula encodes negative motivational value associated with primary punishment in humans. Proc Natl Acad Sci USA 111:11858-11863.

Matsumoto M, Hikosaka O (2009): Representation of negative motivational value in the primate lateral habenula. Nat Neurosci 12:77-84.

Neary TJ, Northcutt RG (1983): Nuclear organization of the bullfrog diencephalon. J Comp Neurol 213:262-278

Northcutt RG (1995): The forebrain of gnathostomes: in search of a morphotype. Brain Behav Evol 46:275-318.

Puelles L, Rubenstein JLR (2003): Forebrain gene expression domains and the evolving prosomeric model. Trends Neurosci 26:469-476.

Puelles L, Milán FJ, Martínez-de-la-Torre M (1996): A segmental map of architectonic subdivisions in the diencephalon of the frog *Rana perezi*: acetylcholinesterase-histochemical observations. Brain Behav Evol 47:279-310.

Pyron RA, Wiens JJ (2011): A large-scale phylogeny of Amphibia including over 2800 species, and a revised classification of extant frogs, salamanders, and caecilians. Mol Phylogenet Evol 61:543-583.

Quina LA, Tempest L, Ng L, Harris JA, Ferguson S, Jhou TC, Turner EE (2015): Efferent pathways of the mouse lateral habenula. J Comp Neurol 523:32-60.

Roth G, Nishikawa KC, Wake DB (1997): Genome size, secondary simplification, and the evolution of the brain in salamanders. Brain Behav Evol 50:50-59.

Schmidt A, Wake MH (1997): Cellular migration and morphological complexity in the caecilian brain. J Morphol 231:11-28.

Stamatakis AM, Stuber GD (2012): Activation of lateral habenula inputs to the ventral midbrain promotes behavioral avoidance. Nat Neurosci 15:1105-1107.

Stephenson-Jones M, Floros O, Robertson B, Grillner S (2012): Evolutionary conservation of the habenular nuclei and their circuitry controlling the dopamine and 5-hydroxytryptophan (5-HT) systems. Proc Natl Acad Sci USA 109:E164-E173.

Villalón A, Sepúlveda M, Guerrero N, Meynard MM, Palma K, Concha ML (2012): Evolutionary plasticity of habenular asymmetry with a conserved efferent connectivity pattern. PLOS One 7:e35329.

Wagner F, Stroh T, Veh RW (2014): Correlating habenular subnuclei in rat and mouse by using topographic, morphological, and cytochemical criteria. J Comp Neurol 522:2650-2662.

441 Yańez J, Anadon R (1994): Afferent and efferent connections of the habenula in the larval sea
442 lamprey (*Petromyzon marinus* L.): an experimental study. J Comp Neurol 345:148-160.
443

Figures

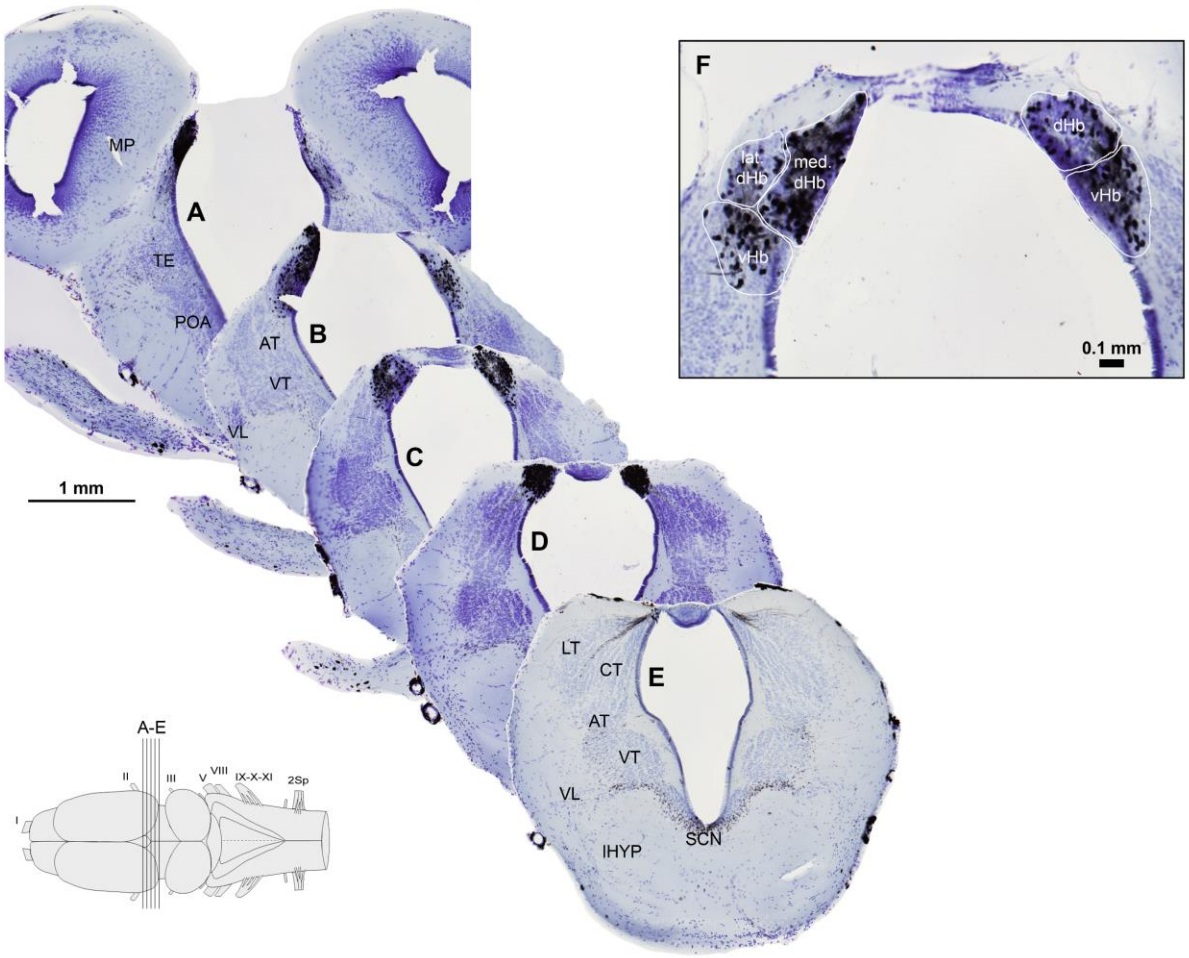

Figure 1. Anatomy of the habenular complex in the fire-belied toad. This specimen (R17) received a large application of biocytin covering part of the ventral tegmentum as well as the dorsoventral extent of the interpeduncular nucleus and rostral raphe median. Retrograde labeling resulting from this application is seen in black, which allowed a clear outline of the extent of the habenular complex. Levels of section in A-E are shown in the lower left inset of a dorsal view of the fire-bellied toad brain. Panel F shows the middle level of the habenular complex between sections B and C at a higher magnification, outlining the different habenular nuclei and their divisions. Damage in the left ventral habenula nucleus in panel B is from a post-fixation artifact.

Abbreviations: AT: anterior thalamic nucleus, CT: central thalamic nucleus, dHb: dorsal habenula nucleus, lat dHb: laterodorsal habenula subnucleus, lHYP: lateral hypothalamic nucleus, LT: lateral thalamic nucleus, med dHb: mediodorsal habenula subnucleus, MP: medial pallium, POA: preoptic area, SCN: suprachiasmatic nucleus, TE: thalamic eminence, vHb: ventral habenula nucleus, VL: ventrolateral thalamic nucleus, VT: ventral thalamic nucleus, 2sp: second spinal nerve.

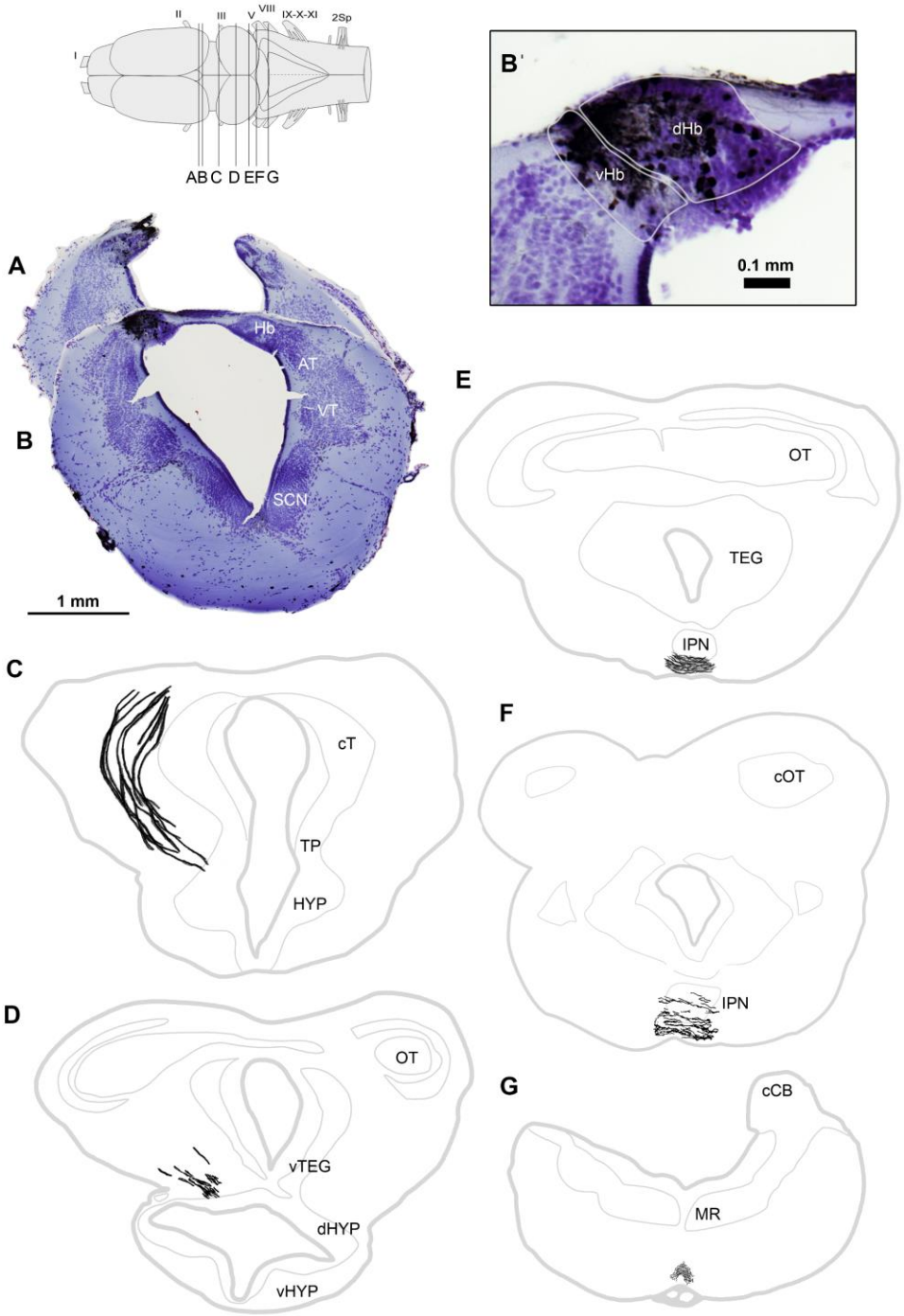

461

462 Figure 2. Representative example of the axonal projection pattern of the habenular complex in

463 the fire-bellied toad. This specimen (Hb7) received an application of biocytin that covered a

464 large part of the left dorsal and ventral nuclei (A-B, B'). Anterograde labeling resulting from this

application is enlarged for clarity (C-G). Levels of section in A-G are shown in the lower left diagram of a dorsal view of the fire-bellied toad brain. Abbreviations: AT: anterior thalamic nucleus, cCB: caudal cerebellum, cT: caudal thalamus, dHb: dorsal habenula nucleus, dHYP: dorsal hypothalamus, Hb: habenula, IPN: interpeduncular nucleus, MR: raphe median, OT: optic tectum, SCN: suprachiasmatic nucleus, TP: posterior tuberculum, vHb: ventral habenula nucleus, vHYP: ventral hypothalamus, VT: ventral thalamic nucleus, vTEG: ventral tegmentum, 2sp: second spinal nerve.

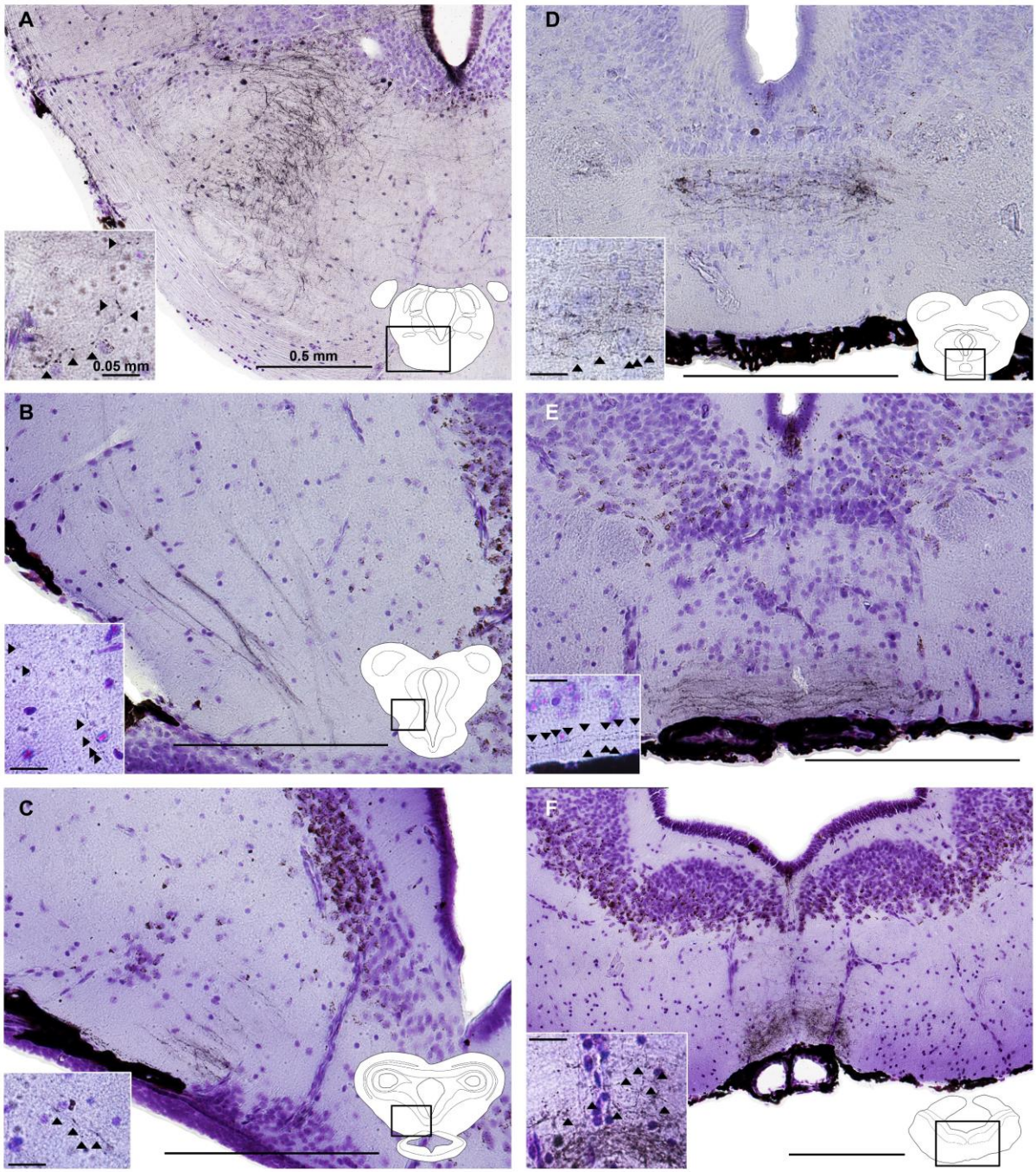

473

474 Figure 3. Axonal projection sites of the habenular complex in the fire-bellied toad. From rostral

475 to caudal, A: Lateral hypothalamus, B: Region of the posterior tuberculum and dorsal

476 hypothalamus, C: Ventral tegmentum, D: Dorsal interpeduncular nucleus, E: Ventral

interpeduncular nucleus, and F: Median raphe. Location of the main micrographs is indicated by boxes on schematic transverse brain sections in the right bottom corner of each panel. Location in panel E is the same as in D, but in a different animal. High power micrographs showing examples of axonal varicosities (arrowheads) are in the insets in the lower left of each panel. Scale bars are 0.5 mm in main micrographs and 0.05 mm in insets. The specimens from which the micrographs were taken are Hb 11 (A), Hb 7 (B and C), Hb 12 (D), Hb 6 (E), and Hb 1 (F). See Table 1 for a full description of axonal projection sites.

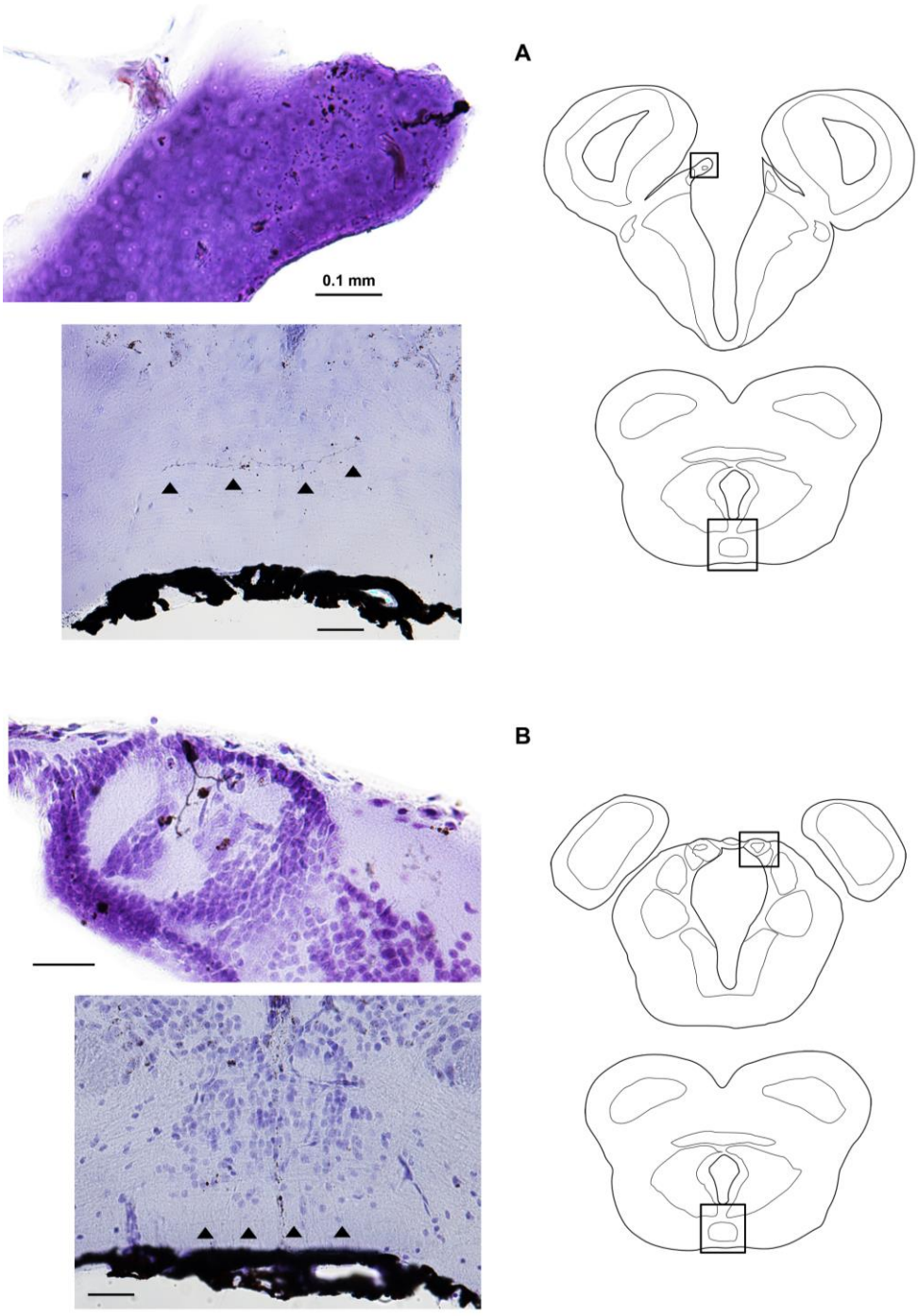

485

486 Figure 4. Intracellular labeling of habenular complex neurons. A: Neuron cell body and proximal
487 dendrite in the rostral part of the left dorsal habenula (top panel) and an axon targeting the dorsal
488 interpeduncular nucleus (arrowheads in bottom panel). B: Two neuron cell bodies in close

proximity and their dendrites in the neuropil of the rostral part of the right dorsal habenula (top panel) and a faintly labeled axon targeting the ventral interpeduncular nucleus (arrowheads in bottom panel). Location of micrographs is indicated by boxes on schematic transverse brain sections in the right column of the figure. The cresyl violet counterstaining procedure did not function properly in A due to wax contamination of the solvent used to prepare the slides. Scale bars are 0.1 mm in all micrographs.

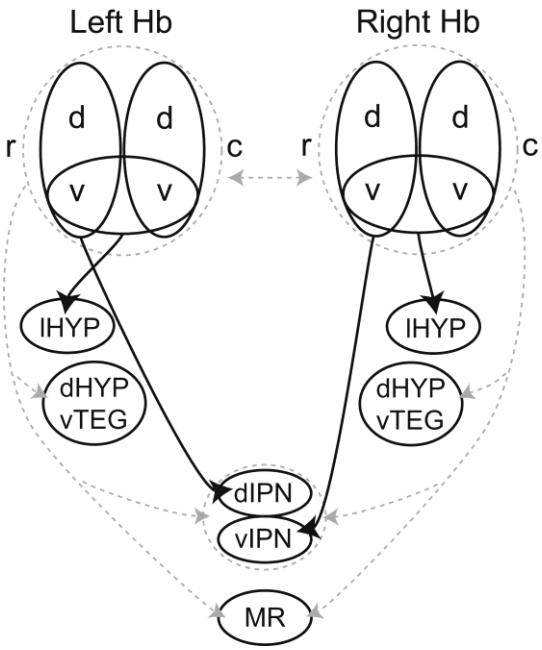

Figure 5. Schematic summary of the efferent axonal projections of the habenular complex in the adult fire-bellied toad. Projections that are shared between nuclei are illustrated using hatched gray lines and circles, while projections tentatively attributed to specific nuclei are illustrated using black lines. In the figure, the rostrocaudal axis of both halves of the habenular complex goes from left to right. The mediolateral axis of the habenula is not shown. Abbreviations: c: caudal, d: dorsal, dHYP: dorsal hypothalamic nucleus, dIPN: dorsal part of the interpeduncular nucleus, Hb: habenula, lHYP: lateral hypothalamic nucleus, MR: raphe median, r: rostral, v: ventral, vIPN: ventral part of the interpeduncular nucleus, vTEG: ventral tegmentum.

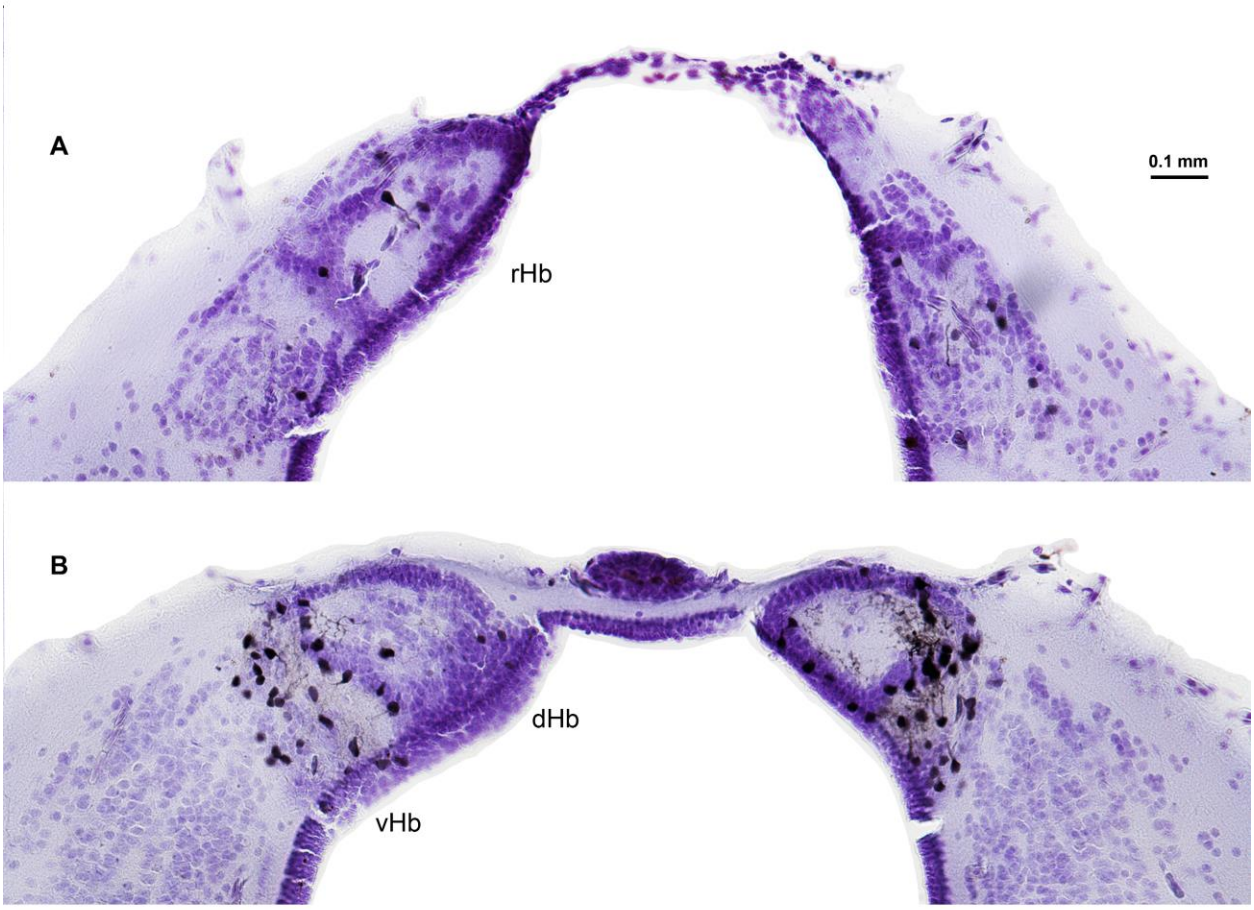

Figure S1. Illustration of the qualitative scale of retrograde labeling intensity used in Table 2. This specimen (R16) received a crystalline biocytin application on the lesioned surface of the interpeduncular nucleus. Panel A shows weak retrograde labeling on both sides of the rostral dorsal and ventral habenular nuclei, with only a few black cell bodies visible. At a middle rostrocaudal level of the habenular complex, panel B shows moderate retrograde labeling on both sides of the dorsal nuclei and strong retrograde labeling on both sides of the ventral nuclei. Abbreviations: dHb: dorsal habenula nucleus, rHb: rostral habenula, vHb: ventral habenula nucleus.


Hb10
Hb14
Hb7
Hb1
Hb14
Hb13
Hb12
Hb11
Hb2
Hb13
Hb8
Hb10
Hb7
Hb1
Hb9
Hb12
Hb2
Hb11
Hb8
Hb7
Hb3
Hb1
Hb11
Hb3
Hb7
Hb1
Hb15
Hb4
Hb7
Hb16
Hb5
Hb15
Hb6
Hb4
Hb12

516

Figure S2. Extent of biocytin applications sites in the habenular complex of the fire-bellied toad. Axonal projections targets of these applications are described in Table 1. Two series of schematic transverse brain sections of the habenular complex and different tones of gray are used to distinguish between application sites of 16 different anterograde tracing experiments. Each experiment involved a different toad. Some applications involved small parts of the medial pallium or underlying thalamic nuclei. Also note that some applications covered a broader rostrocaudal extent of the habenular complex than others. See Figure 1 for approximate levels of section.

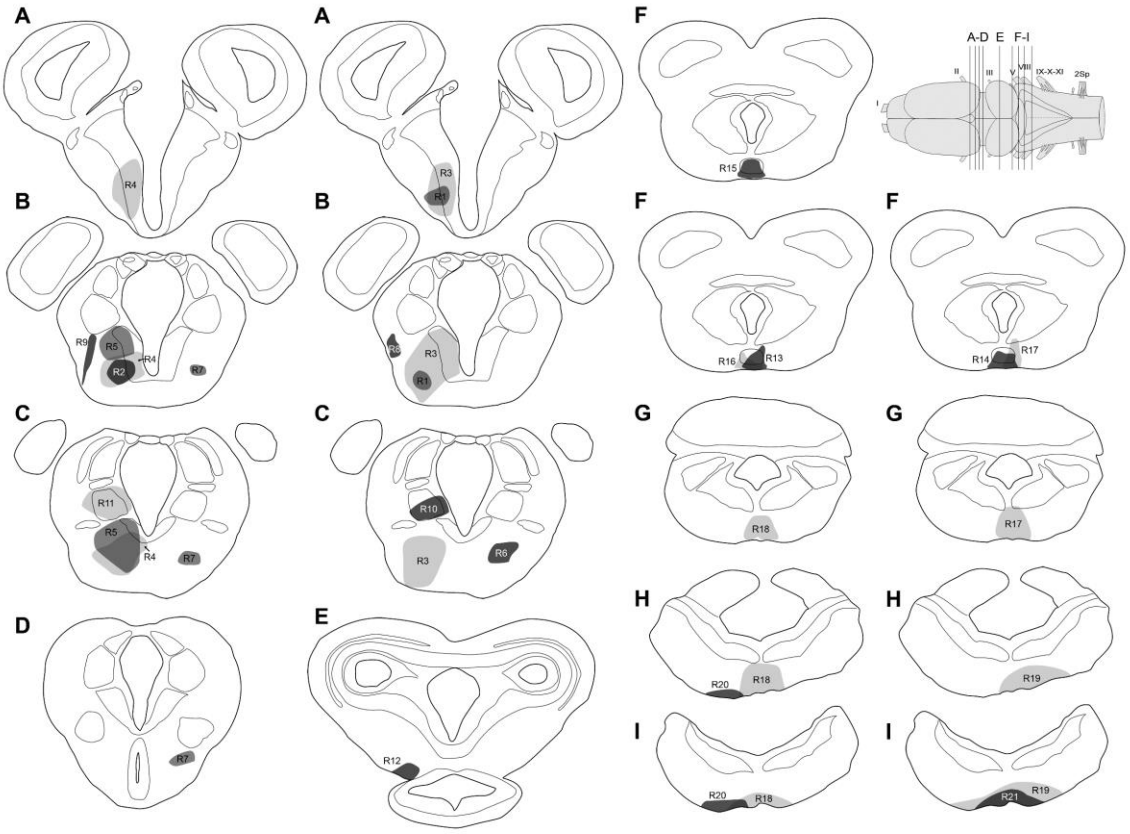

526

527 Figure S3. Extent of biocytin applications sites in brain regions outside of the habenular complex
528 in the fire-bellied toad. Retrograde labeling in the habenular complex following these
529 applications is described in Table 2. Schematic transverse brain sections of the habenular
530 complex and different tones of gray are used to distinguish between application sites of 21
531 different retrograde tracing experiments. Each experiment involved a different toad. Levels of
532 section in A-I are shown in the upper right diagram of a dorsal view of the fire-bellied toad brain.
533 Note that some levels of section are illustrated more than once to show multiple applications
534 targeted to the same general region.

535

Table 1: Axonal projections sites in the brain after biocytin applications to the habenular complex of the fire-bellied toad. Additional regions or tract touched by the applications are indicated in parentheses. Applications to the right habenula are listed above, those to the left below.

ID	Application site	Hb	POA	lHYP	TP/dHYP	mT	cPT	vTEG	IPN	mRaphe
Hb1	right, whole Hb[1] (oht, some AT)	contra (d, v)	+	+	+	+	+	+	+ (+v, d)	+ (v, d)
Hb2	right, rostral Hb				+			+	+ (v)	+ (v)
Hb3	right, mid-dHb (oht, some left POA)	contra (d)						?	+ (v)	+ (v)
Hb4	right, mid-dHb (some oht)	contra (d, v)	+	+	+			+	+ (+v, d)	+ (v)
Hb5	right, caudal dHb (oht)				+			+	+ (v)	+ (v)
Hb6	right, caudal dHb (oht, some caudal vHb)	contra (d)			+			+	+ (v)	+ (v)
Hb7	left, whole Hb (oht)	contra (+/-, d)			+			+	+ (v, d)	+ (v)
Hb8	left, vHb (oht)	contra (d, v)		+	+			+	+ (v, +d)	+ (v, d)
Hb9	left, rostral vHb (oht)	ipsi (+/-, d)			+/-			+/-	-	+/- (v)
Hb10	left, rostral Hb (some MP)	contra (d)		+	+			+	+ (v, d)	+ (v)
Hb11	left, rostral Hb[1] (some AT)	contra (d, +v)	+	+	+	+	+	+	+ (v, +d)	+ (v, d)
Hb12	left, rostral dHb (some CT)	contra (+/-, d)	?	+/-	+	+		+	+ (d)	+ (v)
Hb13	left, rostral dHb (some AT/TE)	contra (d)	+	+	+	+	+	+	+ (v, +d)	+/- (v)
Hb14	left, rostral dHb (some VT and POA)		?	+/-	+	+		+	+ (v, +d)	+/- (v)
Hb15	left, caudal dHb	contra (d, v)			+			+	+ (v)	+ (v)
Hb16	left, caudal dHb (small application)				+			+	+ (v)	+ (v)

[1]Ascending projection to pallium. Legend: +: notable axonal projection, +/-: weak axonal projection, ?: unable to assess if axons make contact in region. Abbreviations: AT: anterior thalamic nucleus, cPT: commissural pretectum, contra: contralateral side of application, CT: central thalamic nucleus, d: dorsal part of brain region, Hb: habenula, HYP: hypothalamus, IPN: interpeduncular nucleus, ipsi: ipsilateral of application, l: lateral part of brain region, MP: medial pallium, mRaphe: raphe median, mT: median thalamic neuropil, oht: olfacto-habenular tract, POA: preoptic area, TE: thalamic eminence, TEG: tegmentum, TP: tuberculum posterius, v: ventral part of brain region, VT: ventral thalamic nucleus.

Table 2: Retrograde labeling in the fire-bellied toad habenular complex after biocytin applications to selected brain regions.

ID	Application site[1]	Application method	Rostral Hb	Middle Hb	Caudal Hb
R1	Left POA + rostral SCN	I	-	-	-
R2	Left rostral SCN	I	-	-	-
R3	Left POA + SCN + lHYP	I	+ (vHb) +/- (dHb)	+ (vHb)	+/- (vHb)
R4	Left POA + SCN + lHYP	I	+ (vHb)	+ (vHb)	+ (vHb)
R5	Left lHYP + SCN (mfb)	I	+ (vHb)	+ (vHb)	-
R6	Right lHYP (mfb)	I	+ (vHb)	+ (vHb)	+/- (vHb)
R7	Right SCN + lHYP	I	+ (vHb)	-	-
R8	Left VL (lfb)	I	-	-	-
R9	Left VL (lfb)	I	-	-	-
R10	Left VT	I	-	-	-
R11	Left VT	I	-	-	-
R12	Left vTEG	C	-	+++	+++
R13	Right IPN (some vTEG)	C	-	+	+++
R14	IPN	C	-	+ (vHb) +/- (dHb)	+++
R15	IPN	C	-	+++ (vHb) + (dHb)	+++
R16	IPN	C	+/-	+++ (vHb) + (dHb)	+++
R17	IPN + vTEG + rostral mRaphe[2]	C	+++ (left dHb) + (vHb, right dHb)	+++	+++
R18	mRaphe	C	+++ (vHb) +/- (dHb)	+++ (vHb) + (dHb)	+++
R19	mRaphe + lMO	C	+++ (vHb) +/- (dHb)	+++ (vHb) + (dHb)	+++
R20	Left, lateral of mRaphe and IPN	C	-	-	-
R21	Caudal mRaphe	C	-	-	-

[1]Note that lHYP and vTEG applications labeled mostly ipsilateral cells in Hb, while applications including IPN or mRaphe labeled cells on both right and left sides in Hb.
[2]Deep lesion that spanned the whole dorsoventral extent of IPN and Raphe.

Legend: +++: strong retrograde labeling, +: moderate, +/-: weak, -: none.

Abbreviations: C: crystalline biocytin application to lesioned brain surface, dHb: dorsal habenula, Hb: habenula, I: iontophoretic injection of biocytin solution, IPN: interpeduncular nucleus, ipsi: ipsilateral side of application, lHYP: lateral hypothalamus, lfb: lateral forebrain bundle was labeled, lMO: lateral medulla oblongata, mfb: medial forebrain bundle was labeled, mRaphe: raphe median, POA: preoptic area, SCN: suprachiasmatic nucleus, vHb: ventral habenula, vTEG: ventral tegmentum, VL: ventrolateral thalamic nucleus, VT: ventral thalamic nucleus.

Table 3: Comparison of main habenular complex axonal projections sites across vertebrates.

Group	Hb division	Axonal target				References
		HYP	TP/vTEG	IPN	Raphe	
Anuran amphibians	vHb (lHb?)	+	+	+[1]	+	present study; Kemali and Làzàr 1985; Kuan et al. 2007
	dHb (mHb?)		+	+[1,2]	+	
Urodele	dHb			+[2]		Kuan et al. 2007
Lampreys	rd/rv Hb (lHb)	+	+			Yańez and Anadon 1994; Stephenson-Jones et al. 2012
	lf/rm Hb (mHb)			+[3]		
Teleost fishes	vHb (lHb)				+	Aizawa et al. 2005; Amo et al. 2010; Villalón et al. 2012
	dHb (mHb)			+[1]		
Lizards	lHb	+	+		+	Distel and Ebbesson 1981; Díaz and Puelles 1992
	mHb			+	+	
Rodents	lHb	+	+	weak	+	Herkenham and Nauta 1979; Kuan et al. 2007; Bianco and Wilson 2008; Kim 2009; Quina et al. 2014
	mHb			+[2]	?	

[1]Left and right Hb target dorsal and ventral IPN, respectively; [2]Symmetric innervation of IPN by left and right Hb; [3]Left and right mHb target rostral and caudal IPN, respectively.

Abbreviations: d: dorsal part of brain region, Hb: habenula, HYP: hypothalamus, IPN: interpeduncular nucleus, l: lateral part of brain region, lf/rm Hb: lamprey left/right middle habenula, m: medial part of brain region, Raphe: raphe median, rd/rv Hb: lamprey right dorsal/ventral habenula, TEG: tegmentum, TP: tuberculum posterius, v: ventral part of brain region.

584